

Diffusive Transport of VOCs through LLDPE and Two Coextruded Geomembranes

Rebecca S. McWatters¹ and R. Kerry Rowe, F.ASCE²

Abstract: The diffusive properties of two coextruded geomembranes, one with a polyamide inner core and the other with an ethylene vinyl-alcohol (EVOH) inner core, and a standard 0.53-mm (20-mil) linear low-density polyethylene (LLDPE) geomembrane were examined. Diffusion and sorption laboratory tests were performed to estimate the parameters controlling diffusive migration, including the partitioning, diffusion, and permeation coefficients of the geomembrane in both the aqueous and vapor phases. Results indicate a significant reduction in mass flux through the coextruded geomembranes compared to conventional LLDPE. The EVOH coextruded geomembrane had the lowest permeation coefficients (P_g) with a range of $(2-6) \times 10^{-12} \text{ m}^2 \text{ s}^{-1}$ for diffusion from the aqueous phase. These values for EVOH are upper bounds and the actual values may be lower than as stated. The polyamide (nylon) coextruded geomembrane had higher values than for EVOH, with a P_g range of $(0.7-2.2) \times 10^{-11} \text{ m}^2 \text{ s}^{-1}$ from the aqueous phase. The highest permeation coefficients were for the standard 20-mil LLDPE, which ranged from $(0.6-1.1) \times 10^{-10} \text{ m}^2 \text{ s}^{-1}$. Thus the permeation coefficient for LLDPE was about one order of magnitude greater than for the nylon coextruded and at least two orders of magnitudes higher than for the EVOH coextruded geomembrane. Both coextruded geomembranes showed decreased P_g values and therefore improved diffusive resistance to volatile organic compounds over traditional 0.56-mm PVC geomembranes. The EVOH geomembrane showed a 5–12-fold decrease in P_g in comparison to a 2.0-mm high density polyethylene geomembrane.

DOI: 10.1061/(ASCE)GT.1943-5606.0000345

CE Database subject headings: Geomembranes; Diffusion; Permeability; Organic compounds; Barriers.

Author keywords: Geomembranes; Diffusion; Permeability; Volatile organic chemicals; Barriers.

Introduction

Geomembrane liners are often used to minimize the migration of both aqueous and vapor phase contaminants found in leachate and landfill gas from municipal and hazardous waste landfills, leachate ponds, and containment basins for fuel and liquid storage. Migration of landfill leachate through the composite bottom liner system has been the primary focus of past research into contaminant transport of volatile organic compounds (VOCs) (Park and Nibras 1993; Xiao et al. 1997; Sangam and Rowe 2001; El-Zein and Rowe 2008). However, migration of VOCs through the landfill cover and the barrier system on side slopes, in both aqueous and vapor phases, can also contribute to atmospheric and groundwater contaminations.

There are two contaminant transport mechanisms relevant to typical landfill applications: advection and diffusion. Either a buildup of leachate head or gas pressure in the landfill provides

the driving force for advective flow through tears or holes in the geomembrane (Stark and Choi 2005; Thusyanthan et al. 2007) or composite liner (Bouazza and Vangpaisal 2006; Bouazza et al. 2008; Saidi et al. 2008; Brachman and Gudina 2008a), particularly when those tears or holes are in a wrinkle (Rowe 1998, 2005; Take et al. 2007; Brachman and Gudina 2008b). However, during the service life of the geomembrane (Rowe 2005; Rowe et al. 2009), even if there are no holes, contaminants such as VOCs can migrate through the nonporous membrane by molecular diffusion (e.g., Haxo 1990; Park and Nibras 1993; Mueller et al. 1998; Rowe 1998, 2005; Sangam and Rowe 2001, 2005; Edil 2003). Thus, the rate of diffusive transport through the geomembrane and its ability to control the release of contaminants needs to be quantified and geomembranes that will best control the contaminant escape to acceptable levels identified.

Common polymers used in barrier systems include high-density polyethylene (HDPE), linear low-density polyethylene (LLDPE), and polyvinyl chloride (PVC) (Park and Nibras 1993; Nefso and Burns 2007). New geomembrane types are also being developed that have the potential for use in landfill cover and liner applications. For example, HDPE geomembranes with added fluorination can be used to reduce VOC diffusion through liners (Sangam and Rowe 2005). The first coextruded multilayer geomembranes had HDPE outer layers and a lower density polyethylene as the inner layer (Kolbasuk 1990). These multilayered geomembranes have evolved to include coextruded geomembranes with polyamide (nylon) as the innermost layer. Polyamides have been shown to have a lower permeability to organic solvents and gases than pure polyethylene resins (Yeh and Fan-Chiang 1996; Gonzalez-Nunez 2001). Most recently, coextruded geomembranes with ethylene vinyl-alcohol (EVOH) layers are

¹Ph.D. Candidate, GeoEngineering Centre at Queen's-RMC, Dept. of Civil Engineering, Queen's Univ., Kingston, ON, Canada K7L 3N6. E-mail: rebecca@ce.queensu.ca

²Vice-Principal (Research), Queen's Univ., Kingston, ON, Canada K7L 3N6; and, Professor, GeoEngineering Centre at Queen's-RMC, Queen's Univ., Kingston, ON, Canada K7L 3N6 (corresponding author). E-mail: kerry@civil.queensu.ca

Note. This manuscript was submitted on December 24, 2008; approved on February 22, 2010; published online on August 13, 2010. Discussion period open until February 1, 2011; separate discussions must be submitted for individual papers. This paper is part of the *Journal of Geotechnical and Geoenvironmental Engineering*, Vol. 136, No. 9, September 1, 2010. ©ASCE, ISSN 1090-0241/2010/9-1167-1177/\$25.00.

also being manufactured to take advantage of the properties of polyethylene as a water barrier while having the potential to substantially reduce the diffusion of VOCs.

The objectives of this paper are to examine the diffusive properties of two coextruded geomembranes (one with a polyamide barrier and one with an ethylene vinyl-alcohol barrier) and to compare the results obtained from previous studies with values for more commonly used cover materials such as LLDPE and PVC. In cover applications, the geomembrane may be either wet (e.g., from condensation) or dry; therefore, consideration is given to diffusion of VOCs from both the aqueous and vapor phases. In addition, the diffusive properties of these coextruded geomembranes and traditional HDPE geomembranes are compared. These comparisons provide as basis for consideration of the potential reduction in diffusive contaminant transport resulting from the potential use of coextruded geomembranes in landfill barrier designs.

Background

Diffusion of vapor or aqueous permeants through geomembranes occurs in three steps: adsorption, diffusion, and desorption (Park and Nibras 1993; Prasad et al. 1994; Sangam and Rowe 2001; Pierson and Barroso 2002; Stark and Choi 2005). First, the contaminant partitions between the source medium and adjacent surface of the geomembrane. Second, the compound diffuses through the geomembrane driven by chemical potential. Finally, the compound partitions between the outer geomembrane surface and the receiving medium (Sangam and Rowe 2001).

When a geomembrane is immersed in a fluid (either gas or liquid) containing a contaminant of interest for sufficient time, equilibrium is reached between the concentration in the geomembrane, c_g (ML⁻³), and the concentration in the fluid, c_f (ML⁻³). The two concentration can be related by Henry's law

$$c_g = S_{gf}c_f \quad (1)$$

where S_{gf} =partitioning coefficient (-).

The diffusive mass flux, f (ML⁻² T⁻¹), of the contaminant through the geomembrane is described by Fick's first law

$$f = -D_g \frac{dc_g}{dz} \quad (2)$$

where the diffusion coefficient, D_g (L² T⁻¹), is specific to the geomembrane and contaminant of interest; c_g =concentration of the compound in the geomembrane (ML⁻³); and z represents the distance parallel to the direction of transport. When the diffusion coefficient is constant, the change in contaminant concentration in the geomembrane with time t is expressed by Fick's second law

$$\frac{\partial c_g}{\partial t} = D_g \frac{\partial^2 c_g}{\partial z^2} \quad (3)$$

The final step is also described by Henry's law

$$c'_g = S'_{gf}c_f \quad (4)$$

The partitioning coefficient into the geomembrane is usually equal to the partitioning coefficient out of the geomembrane ($S_{gf}=S'_{gf}$) when the source and receptor fluid are the same (Sangam 2001).

Since it is very difficult to measure the concentration of contaminant inside the geomembrane, consideration of mass transfer across a geomembrane in terms of the concentration in the fluids

on either side of the geomembrane is used to infer the permeation characteristics of the geomembrane. Substitution of Eq. (1) into Eq. (2) gives

$$f = -D_g \frac{dc_g}{dz} = -S_{gf}D_g \frac{dc_f}{dz} = -P_g \frac{dc_f}{dz} \quad (5)$$

where P_g is the permeation coefficient [L²T⁻¹] and is represented by Eq. (6)

$$P_g = S_{gf}D_g \quad (6)$$

Materials

The study examined two novel coextruded flexible geomembranes and one traditional LLDPE geomembrane supplied by Raven Industries, Engineered Films Division (Sioux Falls, S.D.). Geomembrane No. 1 nylon VBP15 was 0.38-mm (15-mil) thick with a five-layer structure comprised of approximately 42% LLDPE with a 3.5% CaCO₃ inert filler, 6% tie resin (maleic anhydride modified LLDPE), 4% nylon (a polyamide barrier), 6% tie resin, and 42% LLDPE with 3.5% CaCO₃. One LLDPE outer layer was gold in color and the other side was white. The density of geomembrane No. 1 was 920 kg/m³. Geomembrane No. 2 was black and 0.53-mm (20-mil) thick with a five-layer structure comprised of approximately 42% LLDPE, 6% tie resin (maleic anhydride modified LLDPE), 4% ethylene vinyl-alcohol barrier (38 mol % ethylene), 6% tie resin, and 42% LLDPE. Geomembrane No. 3 was a traditional black 0.53-mm (20-mil) thick LLDPE. The polyethylene densities for the second and third geomembranes were 920 kg/m³. Table 1 summarizes relevant properties of the three geomembrane samples.

Benzene, toluene, ethylbenzene, and xylenes (BTEXs) are VOCs commonly found at low concentrations in landfill gas and leachate [e.g., United States Environmental Protection Agency (U.S. EPA) (2003) and Rowe et al. (2004)]. VOC diffusion and sorption tests were performed for these aromatic hydrocarbons from both dilute aqueous and vapor phases. Typical properties are given in Table 2.

Analytical Methods

Samples were analyzed by Purge and Trap gas chromatography/mass spectrometer (P&T)-GC/MS using selective ion monitoring. The procedure used a Hewlett Packard 5890 GC with a P&T unit and 5,972 mass selective detector (MS). The VOC P&T method is based on Environmental Protection Agency (EPA) method 8260 [United States Environmental Protection Agency (U.S. EPA) 1996]. Information about the quality control procedures is detailed in the method outlined by McWatters and Rowe (2007; 2009).

Procedures

A series of sorption and diffusion tests was performed to establish the diffusive characteristics (partitioning, diffusion, and permeation coefficients) for each of the geomembranes. The sorption tests were run in triplicate for each type of geomembrane. In addition, control tests, which did not contain geomembrane samples, were conducted to establish the mass loss of contami-

Table 1. Properties of Geomembranes are Values Provided by the Manufacturer except for Those Marked

Properties	Methods (ASTM)	Units	Values
(a) Properties of nylon VBP15 geomembrane			
Thickness		mm	0.38
Puncture	D4833	Peak (N)	171.5
Tear resistance	D1004	Peak (N)	39.5 × 39.3
Tensile	D6693	Peak (N)	72.7
Load at break	D6693	N	70.1
Elongation at break	D6693	% (min)	608
Tensile strength	D882	N	298
Impact resistance	1709 Method B	g	3,813
Std-OIT ^a		min	18.9
HP-OIT ^a		min	1,450
(b) Properties of 2000B EVOH geomembrane			
Thickness		mm	0.53
Puncture	D4833	Peak (N)	240.6
Tear resistance	D1004	Peak (N)	63.0 × 66.4
Tensile	D6693	Peak (N)	62.3
Load at break	D6693	(N)	60.1
Elongation at break	D6693	% (min)	464
Tensile strength	D882	N	245
Impact resistance	1709 Method B	g	1,350
Std-OIT ^a		min	143
HP-OIT ^a		min	128
(c) Properties of 2000B LLDPE geomembrane			
Thickness		mm	0.53
Puncture	D4833	Peak (N)	194.2
Tear resistance	D1004	Peak (N)	53.9 × 55.0
Tensile	D6693	Peak (N)	129.9
Load at break	D6693	(N)	118.3
Elongation at break	D6693	% (min)	955
Tensile strength	D882	N	407
Impact resistance	1709 Method B	g	2,970
Std-OIT ^a		min	190

^aWhich represent values explicitly obtained in tests performed by the writers.

nants due to sampling procedures or sorption to the cell materials. Diffusion tests for each geomembrane type were run in duplicate or triplicate cells.

Throughout the testing, quality assurance/quality control was monitored with the following procedures. Sample concentrations in the cells were quantified based on a certified BTEX reference standard of known concentration. Surrogate fluorobenzene and 1,4-dichlorobenzene were added to each sample as internal standards and the efficiency of the analytical procedure was calculated based on recovery of these surrogates. Efficiency was required to be within 80–120%. Duplicate and triplicate cell samples at specific time were often analyzed. Blanks, spikes, and quality control samples were run at a frequency of 10%. The GC/MS had a detection limit of 1 µg/L, established prior to testing.

Sorption Tests

For aqueous phase sorption tests, geomembrane samples were immersed in stainless steel cells filled with a dilute aqueous solution of BTEX in water (testing concentrations ranging from 400 to 2,200 µg/L for *m* & *p*-xylenes and from 200 to 1,100 µg/L for benzene, toluene, ethylbenzene, and *o*-xylene) at 24 °C. For the vapor phase sorption tests, geomembrane samples were suspended in the vapor space of the cell above the dilute aqueous solution of BTEX (concentrations ranging from 400 to 4,400 µg/L for *m* & *p*-xylenes and from 200 to 3,000 µg/L for the other contaminants) at 24 °C. Cells were agitated on magnetic stirring plates at a constant temperature of 24 °C. Contaminant concentrations were measured at regular intervals until equilibrium was reached. Some tests were continually sampled beyond equilibrium to monitor for mass loss in the cells over time.

The partitioning coefficient, S_{gf} , for each individual compound was calculated based on rearranging the contaminant mass balance equation at equilibrium [Eq. (7)]

$$M_{s0} = M_{sF} + M_{gF} + M_c \quad (7)$$

where M_{s0} =initial mass of the contaminant in solution (M); M_{sF} =final mass deduced from the measured final concentration of the contaminant in solution (M); M_{gF} =mass contained in the geomembrane inferred from the difference between the initial and final values in solution ($M_{s0} - M_{sF}$) (M); and M_c =mass lost to the system quantified by control tests (M) in terms of S_{gf} as shown in Eq. (8)

Table 2. Selected Properties (from Montgomery and Welkom 1990) of Organic Contaminants Tested

Chemicals	Molar weight (g/mol)	Density (g/cm ³)	Aqueous solubility ^a (mg/L)	log K_{ow}	Coefficient of diffusion in water ^b (m ² /s)	Coefficient of diffusion in air ^b (m ² /s)	Henry's constant ^b k [L (water)/L (air)]	Initial	Initial
								concentration in aqueous tests, ^c c_{f0} (µg/L)	concentration in vapor tests, ^c c_{f0} (µg/L)
Benzene	78.11	0.8765	1,780	2.13	11.0 × 10 ⁻¹⁰	9.6 × 10 ⁻⁶	0.218	200–1100	200–3,000
Toluene	92.14	0.8669	515	2.79	9.4 × 10 ⁻¹⁰	8.5 × 10 ⁻⁶	0.258	200–1100	200–3,000
Ethylbenzene	106.17	0.8670	152	3.13	8.5 × 10 ⁻¹⁰	7.7 × 10 ⁻⁶	0.305	200–1100	200–3,000
<i>m</i> -xylene	106.17	0.8642	162	3.20	8.5 × 10 ⁻¹⁰	7.7 × 10 ⁻⁶	0.290	400–2200	400–4,400
<i>p</i> -xylene	106.17	0.8811	156	3.13	8.5 × 10 ⁻¹⁰	7.7 × 10 ⁻⁶	0.290	400–2200	400–4,400
<i>o</i> -xylene	106.17	0.8802	152	3.18	8.5 × 10 ⁻¹⁰	7.6 × 10 ⁻⁶	0.201	200–1100	200–3,000

^aAt 20 °C.

^bFrom Tucker and Nelken (1982) at infinite dilution at 24 °C.

^cInitial concentration in the aqueous phase for the aqueous and vapor diffusion and sorption tests.

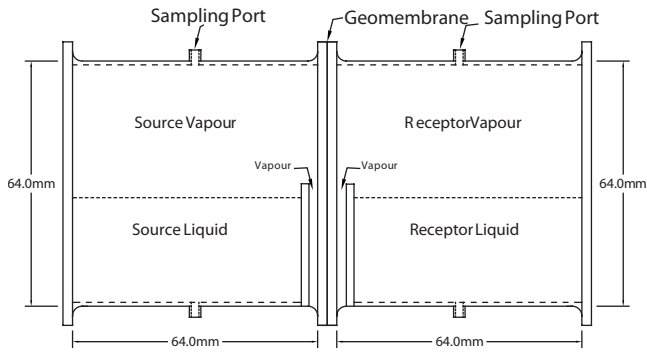


Fig. 1. Schematic of an aqueous-vapor/vapor-aqueous diffusion cell

$$S_{gf} = \frac{[c_{f0}V_{f0} - c_{fF}V_{fF} - M_c]\rho_g}{M_g c_{fF}} \quad (8)$$

where c_{f0} =initial contaminant concentration in solution (ML^{-3}); V_{f0} =initial solution volume (L^3); c_{fF} =final contaminant concentration in solution (ML^{-3}); V_{fF} =final solution volume (L^3); M_g =initial mass of the geomembrane sample (M); ρ_g =geomembrane density (ML^{-3}); and c_{gF} =final concentration of the contaminant in the geomembrane at equilibrium (ML^{-3}).

Aqueous Diffusion Tests

Stainless steel double compartment cells (source and receptor) were employed in aqueous phase diffusion tests. The geomembrane sample was secured between the source and receptor compartments. The source was filled with a dilute aqueous BTEX solution (concentrations ranging from 400 to 2,200 $\mu\text{g}/\text{L}$ for *m* & *p*-xylenes and from 200 to 1,100 $\mu\text{g}/\text{L}$ for the other contaminants) while the receptor was filled with deionized water. Cells were agitated on magnetic stirrers and maintained at 24°C. The source and receptor were sampled regularly and frequently until either equilibrium was reached or for the first 20 days of the testing period. The frequency of sampling decreased as tests proceeded for longer periods of time to prevent wear on the septums leading to mass loss in the cell. Since these samplings were performed at greater intervals, triplicate samples were taken to confirm an accurate assessment of the concentration in both the source and receptor.

Vapor Diffusion Tests

Vapor diffusion tests employed a modified stainless steel double compartment (source and receptor) cell as shown in Fig. 1. Within the source compartment, there was a steel partition that kept the liquid phase section (aqueous solution) away from the geomembrane and allowed a vapor phase to exist both above the liquid and adjacent to the entire geomembrane (Fig. 1). The receptor had a similar setup. When the tests were running, the cell was positioned horizontally, such that the geomembrane sample, secured between the source and receptor, was only exposed to the vapor phase. As in the aqueous diffusion tests, a dilute aqueous BTEX solution (concentrations as per vapor sorption tests) was introduced to the source liquid chamber and the contaminants were allowed to equilibrate between the aqueous and vapor phases of the source compartment at 24°C. Preliminary tests conducted prior to the diffusion tests indicated that equilibrium between the aqueous and vapor phases in the source was achieved in about 0.5 h or less, therefore the time to reach equilibrium in all tests was

taken as 1 h. Studies involving the distribution of volatile contaminants between water and air found a similar time to equilibrium (Peng 1998). The receptor liquid was de-ionized water.

Liquid samples were taken from the aqueous phase and analyzed by P&T GC/MS. The vapor phase concentrations were then calculated from the liquid concentrations using Henry's law. Preliminary tests were performed to confirm the validity of Henry's law relation using P&T (for analysis of liquid phase contaminants) and solid-phase microextraction (for analysis of vapor phase contaminants). For the diffusion tests, liquid phase samples were taken as P&T GC/MS was the preferred method of analysis as it is a well established method used in several EPA procedures for VOC detection including EPA method 8260 [United States Environmental Protection Agency (U.S. EPA) 1996]. As in the aqueous diffusion tests, the frequency of sampling decreased over time to minimize mass losses from the cell.

The tests were designed such that the geomembrane sample was exposed solely to the vapor phase, however, condensation of water vapor onto the geomembrane was possible. The majority of tests did not have condensation. However, in some cases, condensation was noted on both sides of the geomembrane. When this occurred, it usually took the form of small droplets of water covering less than half of the geomembrane surface. In a few cases, there was a thin water layer covering the entire surface of the geomembrane. Multiple diffusion tests for each geomembrane type were performed to account for some of the variability in results for the variable condensation. The case with a full condensation film effectively becomes an aqueous phase test once the full film is developed, but in these cases, the test probably involves diffusion from the vapor phase in the early stages and diffusion from the aqueous phase in later stages of the test. Condensation in the tests is similar to that which may be expected in a landfill where the migration of contaminants through the geomembrane is thought to occur by one of the two scenarios: (a) vapor phase contaminants partitioning between the vapor and geomembrane where there is no condensation and (b) vapor phase contaminants partitioning into the water condensate and then into the geomembrane where condensation is present. A combination of the two scenarios would be most likely to exist in field conditions where the geomembrane, resting on unsaturated soil, is exposed to both gas filled and water filled pores.

Modeling Diffusion

The diffusion (D_g), partition (S_{gf}), and permeation (P_g) coefficients for BTEX contaminants and the geomembranes were calculated as per the method outlined by Rowe et al. (1995a). Theoretical curves are fit to experimental data using the finite layer analysis program POLLUTE v.7 (Rowe and Booker 2004). The method is based on concepts and theory first developed by Rowe et al. (1988) and Barone et al. (1992) for clay soils and by Rowe et al. (1995b, 2004) for geomembranes. For the vapor phase tests, the partitioning (S_{gf}) and permeation coefficients (P_g) were calculated with respect to the concentration in the aqueous phase to allow direct comparison with the values deduced from the aqueous phase tests. The partitioning coefficients with respect to the concentration in the vapor phase can be calculated from Henry's law

$$S_{gf}^* = k S_{gf} \quad (9)$$

and

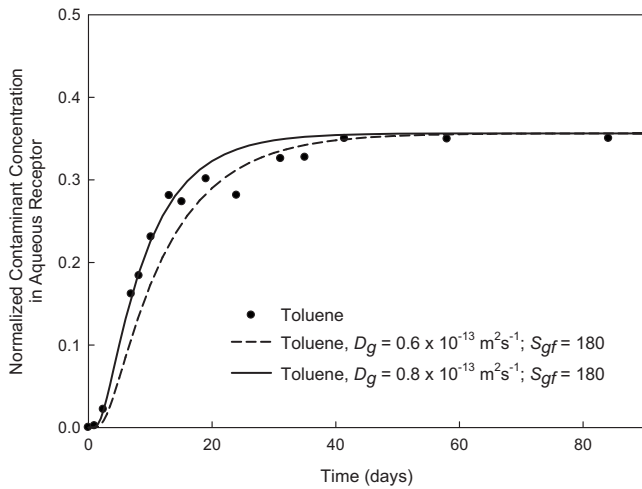


Fig. 2. Toluene concentration changes in the receptor during aqueous diffusion tests using coextruded nylon GM

$$P_g^* = kP_g \quad (10)$$

where S_{gf}^* and P_g^* = partitioning and permeation coefficients relative to the concentration in the vapor phase (-) and k = Henry's law coefficient specific to each contaminant and temperature (-) given in Table 2.

Results

Nylon VBP15 Geomembrane

Contaminant concentrations in the cell (sorption tests) and in the source and receptor (diffusion tests) were monitored with time until equilibrium was reached. The results from the sorption tests were used to obtain an estimate of the partitioning coefficient, S_{gf} , used in interpreting the diffusion tests. Typical theoretical curves obtained with POLLUTE v.7 (Rowe and Booker 2004) are shown together with the experimental data in Figs. 2–4. The D_g , S_{gf} , and P_g coefficients for each contaminant were calculated by fitting the theoretical curves to the experimental data. Given the scatter of

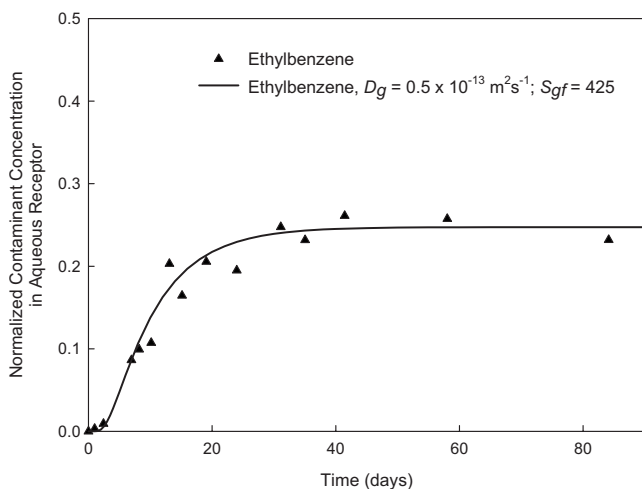


Fig. 3. Ethylbenzene concentration changes in the receptor during aqueous diffusion tests using coextruded nylon GM

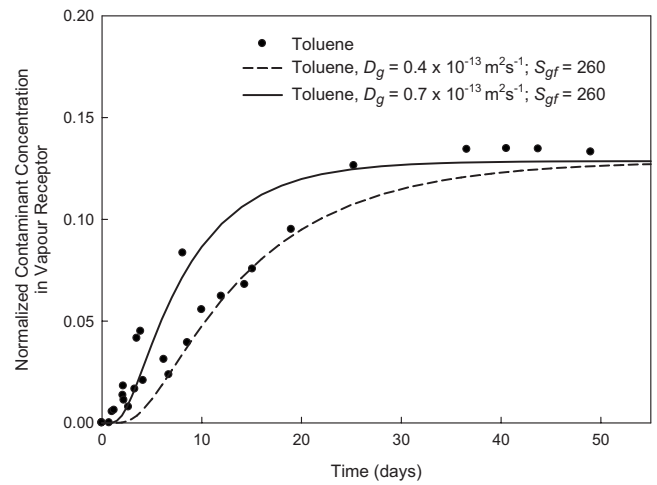


Fig. 4. Toluene concentration changes in the receptor during vapor diffusion tests using coextruded nylon GM

the data, there was generally a range of parameters that could reasonably explain the data and that range is shown. To minimize scatter in the data, triplicate samples from the cells were used together with analytical quality assurance/quality control checks to eliminate outliers.

Fig. 2 shows the increase in toluene concentration in the receptor solution for an aqueous diffusion test. The changes in concentration are plotted as normalized concentrations relative to the initial source concentration. The equilibrium concentration was reached after 40 days. Toluene source concentration decreased by 60% of the initial concentration. The partitioning coefficient was 180 and the diffusion coefficient ranged between $(0.6\text{--}0.8) \times 10^{-13} \text{ m}^2 \text{ s}^{-1}$ with the range being a result of the scatter of the experimental data points. Fig. 3 shows a similar change in receptor concentration for ethylbenzene, which had a partitioning coefficient of 425 and a diffusion coefficient of $0.5 \times 10^{-13} \text{ m}^2 \text{ s}^{-1}$. The concentration decrease in the source was 70%.

For diffusion tests in the vapor phase, the concentrations of contaminants were measured in the source and receptor aqueous phases. Vapor concentrations were correlated from aqueous sample concentrations and plotted. Fig. 4 shows the toluene concentration changes over time in the receptor (normalized relative to the initial concentration of contaminants in the source vapor reservoir) during the diffusion tests. In repeated tests, equilibrium was reached after 35–40 days. For toluene, the vapor partitioning parameter was 260 and the diffusion coefficient ranged from $(0.4\text{--}0.7) \times 10^{-13} \text{ m}^2 \text{ s}^{-1}$. Table 3 presents all three diffusive migration parameters— D_g , S_{gf} , and P_g —of all contaminants in both the aqueous and vapor phases through the coextruded nylon geomembrane.

2000B LLDPE Geomembrane

Sorption and diffusion tests in the aqueous and vapor phases were performed in the same manner for 2000B LLDPE geomembrane samples. Fig. 5 shows the decrease in normalized (with respect to the initial source concentration) *o*-xylene concentrations in the source solution, while Fig. 6 shows the increase in normalized *o*-xylene concentrations in the receptor solution. The equilibrium concentration was reached after 25 days. *o*-Xylene concentrations decreased by 80% of the initial concentration. These two figures illustrate (a) the variability of data in the source and receptor that

Table 3. Inferred Partitioning, Diffusion, and Permeation Coefficients of Coextruded Nylon VBP15 Geomembranes from Diffusion Tests in the Aqueous and Vapor Phase

Contaminant	Nylon VBP15 aqueous results			Nylon VBP15 vapor results				
	S_{gf} (-)	D_g (10^{13} m ² s ⁻¹)	P_g (10^{10} m ² s ⁻¹)	S_{gf} (-)	D_g (10^{13} m ² s ⁻¹)	P_g (10^{10} m ² s ⁻¹)	S_{gf}^* (-)	P_g^* (10^{10} m ² s ⁻¹)
Benzene	120	0.6–0.8	0.07–0.10	150	0.5–0.8	0.08	30	0.02
Toluene	180	0.6–0.8	0.11–0.14	260	0.4–0.7	0.10–0.13	70	0.02–0.03
Ethylbenzene	425	0.5	0.21	485	0.3–0.8	0.15–0.24	150	0.05–0.07
<i>m</i> & <i>p</i> -xylenes	430	0.5	0.22	495	0.3–0.5	0.19–0.25	145	0.06–0.07
<i>o</i> -xylene	400	0.5	0.20	440	0.3–0.5	0.13–0.22	90	0.03–0.04

Note: For vapor phase tests, S_{gf} is calculated relative to the concentration in the aqueous phase for direct comparison with the aqueous phase test results. The partitioning and permeation coefficients S_{gf}^* and P_g^* relative to the concentration in the vapor phase can be calculated from $S_{gf}^* = kS_{gf}$ and $P_g^* = kP_g$ where Henry's coefficient k is given in Table 2.

results from analytical methods and the corresponding range of uncertainty with respect to the diffusion coefficient and (b) the relatively well-defined partitioning coefficient associated with the final equilibrium concentrations. The data presented are within the variability limits of the analytical method and are well above the detection limits of 1 $\mu\text{g/L}$ for the P&T GC/MS method. Scatters in the data are attributed to slight changes in sampling

volumes (1–2 μL), temperature ($\pm 1^\circ\text{C}$), and performance of the GC/MS. Table 4 presents all three diffusive migration parameters— D_g , S_{gf} , and P_g —of all contaminants in both the aqueous and vapor phases through the standard LLDPE geomembrane. These values can be compared to those for the nylon geomembrane (Table 3).

2000B EVOH Geomembrane

The partitioning coefficients S_{gf} for the coextruded 2000B EVOH geomembrane are presented in Table 5. A noncorrected S_{gf} was calculated assuming that there was no significant mass loss of contaminants. This case assumes that the sorption of contaminants to the testing material (glass vials or cells) is negligible in comparison to their attraction to the geomembrane. The corrected S_{gf} took into consideration the mass loss of contaminants to the testing material as evident in the control tests (this represents an upper bound to the loss since there was no geomembrane present in the control tests and given the option of sorption to geomembrane as opposed to the cell materials in the sorption tests the loss to the cell is expected to be equal to or less than in the control tests). Thus the actual values for the partitioning coefficients are expected to lie between the noncorrected and corrected values. It is noted that the differences between the corrected and uncorrected values are quite small (Table 5).

The highest corrected S_{gf} value for the aqueous phase was 670 for ethylbenzene, followed by *m* & *p*-xylenes ($S_{gf}=560$), *o*-xylene ($S_{gf}=495$), toluene ($S_{gf}=309$) and benzene ($S_{gf}=165$). The vapor phase S_{gf} values followed a similar trend of ethylbenzene ($S_{gf}=603$), *m* & *p*-xylenes ($S_{gf}=509$), *o*-xylene ($S_{gf}=425$), toluene ($S_{gf}=216$), and benzene ($S_{gf}=75$).

Diffusion tests were also carried out for the coextruded 2000B EVOH geomembrane. Concentrations in the source decreased with time, reaching an apparent equilibrium after 35 days (Fig. 7). We say apparent equilibrium because this represents diffusion into the LLDPE upper layers with the EVOH layer acting as an apparent, on the time scale of the test today, impermeable layer and so there is negligible mass transfer to the LLDPE or receptor cell below the EVOH layer (Fig. 8). Concentrations in the receptor were below detection limits in some tests and very small to negligible in other tests (the maximum concentration data point is only about 3–11% of the original source concentration depending on the contaminant). If the tests are run long enough, there should be a second, ultimate, equilibrium once there is sufficient time for diffusion through the EVOH layer. Since the concentration in the receptor after 720 days (i.e., at the time of writing) was at or below the detection limit, it is not possible to precisely define the diffusion properties of the EVOH layer at this time. Conse-

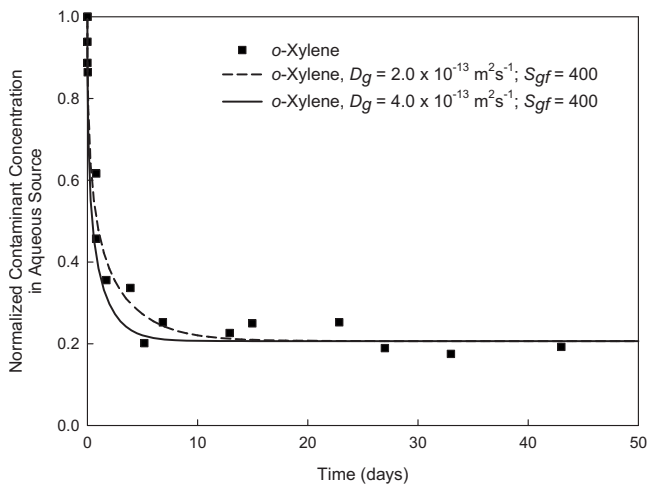


Fig. 5. *o*-xylene concentration changes in the source during aqueous diffusion tests using LLDPE GM

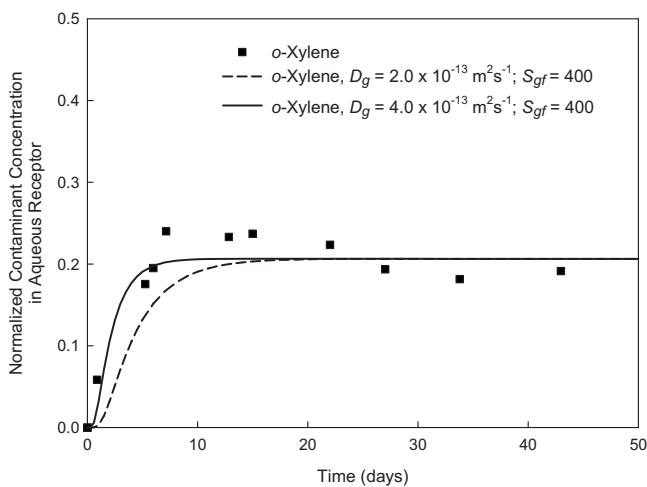


Fig. 6. *o*-Xylene concentration changes in the receptor during aqueous diffusion tests using LLDPE GM

Table 4. Inferred Partitioning, Diffusion, and Permeation Coefficients of 2000B LLDPE Geomembranes from Diffusion Tests in the Dissolved and Vapor Phase

Contaminant	LLDPE (20-mil) aqueous results			LLDPE (20-mil) vapor results				
	S_{gf} (-)	D_g (10^{13} m ² s ⁻¹)	P_g (10^{10} m ² s ⁻¹)	S_{gf} (-)	D_g (10^{13} m ² s ⁻¹)	P_g (10^{10} m ² s ⁻¹)	S_{gf}^* (-)	P_g^* (10^{10} m ² s ⁻¹)
Benzene	180	4.0	0.7	150	4.0	0.6	33	0.1
Toluene	350	3.0	1.1	300	2.5	0.8	80	0.2
Ethylbenzene	420	2.0	0.8	420	2.5	1.1	130	0.3
<i>m</i> & <i>p</i> -xylenes	445	2.0	0.9	440	2.0	0.9	130	0.3
<i>o</i> -xylene	400	2.0	0.8	375	2.0	0.8	75	0.2

Note: For vapor phase tests, S_{gf} is calculated relative to the concentration in the aqueous phase for direct comparison with the aqueous phase test results. The partitioning and permeation coefficients S_{gf}^* and P_g^* relative to the concentration in the vapor phase can be calculated from $S_{gf}^* = kS_{gf}$ and $P_g^* = kP_g$ where Henry's coefficient k is given in Table 2.

quently, upper bound permeation coefficients were obtained by fitting the diffusion curves to the most recent (highest) concentrations detected in the receptor for each compound. It is expected that as cells continue to be tested the concentrations in the receptor will remain low or negligible. If this is the case, the upper bound permeation coefficients will decrease. Concentrations in the source are continually monitored to ensure equilibrium is maintained and there is no mass loss through sampling ports.

The five-layer geomembrane was modeled as three layers treating the thin tie resin layers (a thin modified LLDPE) as part of the LLDPE layers. Contaminants were analyzed as they migrated through LLDPE (first layer), then through the ethylene vinyl-alcohol barrier (second layer), and finally through another LLDPE layer (third layer). The LLDPE and EVOH layers had different partitioning and diffusion coefficients. Partitioning coefficients (Table 5) were established based on both the sorption tests for the EVOH geomembrane (e.g., $S_{gf}=500$ for *o*-xylene) and from the fit to the apparent equilibrium concentration in the source reservoir in the diffusion test (e.g., $S_{gf}=550$ for *o*-xylene) and the fits for *o*-xylene using the two different estimates of S_{gf} are shown in Fig. 7. The partitioning coefficients given in Table 5 are for the multilayered coextruded geomembrane. Because of the dominate role played by the other layers, with the EVOH layer being only 4% of the geomembrane thickness, it was not possible to separately evaluate S_{gf} and D_g for the thin EVOH layer and only the permeation coefficient could be calculated for the EVOH layer by fitting the theoretical curves to the receptor cell data (e.g., see Fig. 8) to give the values shown in Table 6.

A single layer approach to modeling the diffusion tests was also examined since it would greatly simplify modeling field cases. This approach used the partitioning coefficients deduced as described above and given in Table 5 together with a diffusion coefficient for the entire layer that gave a good "upper bound"

match to the receptor concentration data. Since in reality only half the geomembrane is contributing to sorption in the diffusion tests to date, this single layer approach did not model the concentration drop in the source cell as well as the three layer approach described above; however, it gave similar results for the receptor as the more rigorous three layer model and is expected to be adequate for modeling mass transfer in landfill covers given the other uncertainties. Table 7 summarizes the values of D_g , S_{gf} , and P_g (for the entire layer) that can be used to model the mass flux through the EVOH geomembrane as a single layer.

Diffusion tests in the vapor phase showed similar results to those in the aqueous phase tests discussed above. Concentrations in the source decreased with time, reaching apparent equilibrium after about 30 days. Concentrations in the receptor were either below detection limits or very low and hence upper bound parameters were established based on the latest/highest value "detected." Again it is expected that the concentrations in the receptor will remain low or negligible for considerable time into the future, ultimately leading to a smaller upper bound values than presently given.

When the geomembrane was modeled as a three layer system, the upper bound vapor phase permeation coefficients given in Table 6 were estimated for the thin EVOH layer (with the LLDPE layers being modeled with the partitioning coefficients given in Table 5). Upper bound fits to the receptor data were obtained using the vapor phase parameters for the entire geomembrane thickness, as given in Table 7.

Diffusion coefficients for the LLDPE and coextruded nylon geomembrane obtained from aqueous and vapor phase diffusion tests were very similar. This coincides with the previous study of PVC geomembranes (McWatters and Rowe 2009) where it was concluded that diffusion coefficients are essentially identical for the aqueous and vapor phase contaminant migration. Once the

Table 5. Estimated Partitioning Coefficients, S_{gf} , of Coextruded EVOH Geomembrane from Sorption Tests

Contaminants	Aqueous phase S_{gf} results			Vapor phase S_{gf} results		
	Noncorrected sorption tests	Corrected sorption tests	Inferred from diffusion tests	Noncorrected sorption test	Corrected sorption test	Inferred from diffusion tests
Benzene	167	165	200	76	75	85
Toluene	312	309	350	218	216	200
Ethylbenzene	675	670	700	608	603	670
<i>m</i> & <i>p</i> -xylenes	563	560	600	513	509	560
<i>o</i> -xylene	500	495	550	427	425	495

Note: For vapor phase tests, S_{gf} is calculated relative to the concentration in the aqueous phase for direct comparison with the aqueous phase test Results. The partitioning and permeation coefficients S_{gf}^* and P_g^* relative to the concentration in the vapor phase can be calculated from $S_{gf}^* = kS_{gf}$ and $P_g^* = kP_g$ where Henry's coefficient k is given in Table 2.

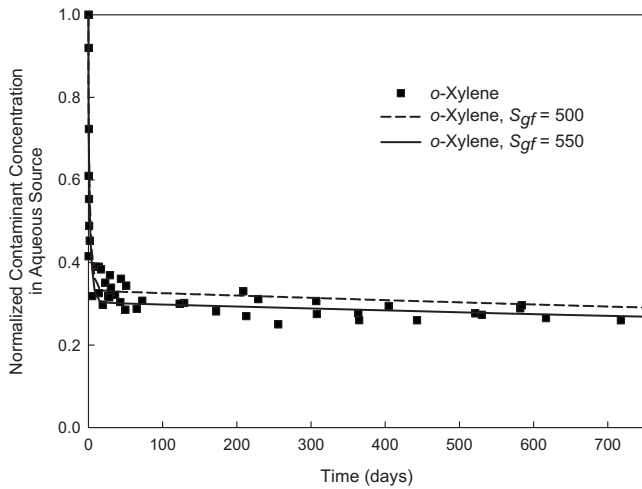


Fig. 7. *o*-Xylene concentration changes in the source during aqueous diffusion tests using coextruded EVOH GM and upper bound theoretical fits to the data

contaminant has partitioned into the geomembrane, the source medium has no influence on transport. Diffusion is primarily controlled by the polymer matrix. In the case of the EVOH coextruded geomembrane, upper bound diffusion coefficients obtained from vapor tests were roughly half the value of coefficients obtained from aqueous tests, although in both cases, these concentrations were very low and sometimes close to detection limits. Vapor diffusion tests typically experience more mass loss due to BTEX sorbing to the testing apparatus than aqueous tests; therefore, when the amount of BTEX migrating to the receptor is already very limited, this mass loss impacts concentrations levels.

The mass transfer across the geomembrane boundary is represented by the permeation coefficient, P_g . The calculated single layer P_g values for the three geomembranes tested were compared with P_g values from previous tests using a 0.76-mm thick PVC geomembrane (McWatters and Rowe 2009) and (2.0-mm) thick HDPE geomembrane (Sangam and Rowe 2001). The ratios of P_g

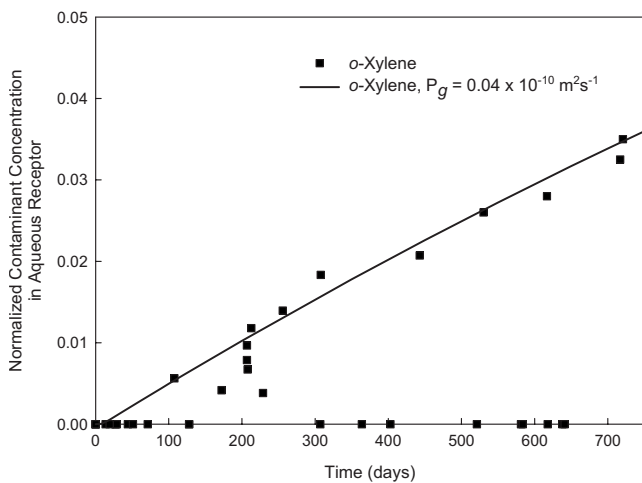


Fig. 8. Upper bound *o*-xylene concentration changes in the receptor during aqueous diffusion tests using coextruded EVOH GM (note that the very small numbers are within the range of uncertainty related to detection limits)

Table 6. Inferred Upper Bound Permeation Coefficients for the EVOH Layer Component of the 2000B EVOH Geomembrane in the Aqueous and Vapor Phases

Contaminants	P_g	P_g	P_g^*
	Aqueous phase ($10^{12} \text{ m}^2 \text{ s}^{-1}$)	Vapor phase ($10^{12} \text{ m}^2 \text{ s}^{-1}$)	Vapor phase ($10^{12} \text{ m}^2 \text{ s}^{-1}$)
Benzene	0.90	0.45	0.009
Toluene	0.85	0.42	0.011
Ethylbenzene	0.80	0.40	0.012
<i>m</i> & <i>p</i> -xylenes	0.80	0.37	0.011
<i>o</i> -xylene	0.75	0.37	0.007

Note: For vapor phase tests, P_g is calculated relative to the concentration in the aqueous phase for direct comparison with the aqueous phase test results. The permeation coefficients P_g^* relative to the concentration in the vapor phase can be calculated from $P_g^* = kP_g$ where Henry's coefficient k is given in Table 2.

for PVC over P_g of the specified geomembrane are presented in Tables 8 and 9 for the aqueous and vapor phases, respectively.

The PVC to LLDPE P_g ratio was 3–12 for the aqueous phase and 1–5 for the vapor phase. The ratio of P_g of PVC to the nylon geomembrane ranged from 20 to 45 in the aqueous phase and 10–45 in the vapor phase. The data indicate a significant increase in the relative performance of the nylon geomembrane in reducing the mass flux when compared to PVC. The geomembrane with the EVOH barrier showed the greatest improvement in reducing the mass flux of BTEX. The upper bound P_g values of EVOH were 110–200 times smaller than for PVC. For the vapor phase the ratios were 225–360. Even with the upper bound permeation values, it is apparent that the EVOH performs as a much better diffusive barrier than PVC and LLDPE. The relative performance of EVOH is likely even better than implied by the upper bound values obtained in this paper.

Diffusion coefficients for each of the geomembrane types studied were compared with results from a previous study of a traditional 2.0-mm thick HDPE geomembrane (Sangam and Rowe 2001). Results from aqueous phase diffusion tests are presented in Table 10. Both coextruded geomembranes have notably lower diffusion coefficients than all the other geomembranes, including HDPE. Coextruded EVOH has a range of $(0.075\text{--}0.09) \times 10^{-13} \text{ m}^2 \text{ s}^{-1}$ versus $(1.5\text{--}3.5) \times 10^{-13} \text{ m}^2 \text{ s}^{-1}$ for HDPE for the diffusion coefficient.

Permeation coefficients for each of the geomembranes are compared in Table 11. HDPE and the nylon coextruded geomembrane have similar permeation coefficient values for ethylbenzene and xylenes [$(0.4\text{--}0.6) \times 10^{-10} \text{ m}^2 \text{ s}^{-1}$], while HDPE proves to provide a better diffusive barrier to benzene and toluene [$(0.1\text{--}0.3) \times 10^{-10} \text{ m}^2 \text{ s}^{-1}$ for HDPE versus $(0.6\text{--}0.8) \times 10^{-10} \text{ m}^2 \text{ s}^{-1}$ for nylon]. For the coextruded EVOH geomembrane, the permeation coefficients [$(0.02\text{--}0.06) \times 10^{-10} \text{ m}^2 \text{ s}^{-1}$] are smaller than for HDPE, a factor of between 5 and 12 (depending on the contaminant).

Results from this study indicate that coextruded geomembranes with a polyamide or ethylene vinyl-alcohol barrier can reduce the diffusive mass flux of BTEX compounds through barrier systems substantially in comparison to traditional LLDPE and PVC materials. The coextruded EVOH geomembranes can also reduce the diffusive mass flux of BTEX compounds compared with the standard HDPE geomembranes most commonly used in landfill design. It is specifically the EVOH layer in the geomembrane that has the potential to improve landfill systems in terms of

Table 7. Approximate Upper Bound Parameters in the Aqueous and Vapor Phases for Modeling the Entire 2000B EVOH Geomembrane as a Single Layer System

Contaminant	Aqueous phase			Vapor phase				
	S_{gf} (-)	D_g (10^{13} m ² s ⁻¹)	P_g (10^{10} m ² s ⁻¹)	S_{gf} (-)	D_g (10^{13} m ² s ⁻¹)	P_g (10^{10} m ² s ⁻¹)	S_{gf}^* (-)	P_g^* (10^{10} m ² s ⁻¹)
Benzene	200	0.09	0.018	85	0.045	0.004	20	0.001
Toluene	350	0.085	0.030	200	0.042	0.008	50	0.002
Ethylbenzene	700	0.080	0.056	670	0.040	0.027	205	0.001
<i>m</i> & <i>p</i> -xylenes	600	0.080	0.048	560	0.037	0.021	160	0.006
<i>o</i> -xylene	550	0.075	0.041	495	0.037	0.018	100	0.003

Note: For vapor phase tests, S_{gf} is calculated relative to the concentration in the aqueous phase for direct comparison with the aqueous phase test results. The partitioning and permeation coefficients S_{gf}^* and P_g^* relative to the concentration in the vapor phase can be calculated from $S_{gf}^* = kS_{gf}$ and $P_g^* = kP_g$ where Henry's coefficient k is given in Table 2.

containing VOC contaminants commonly found in MSW landfills. Further studies on the diffusive properties of the single layer of 0.02-mm-thick EVOH are in progress. There is the potential to combine the desired properties of both EVOH and HDPE in a novel coextruded geomembrane.

For now, engineers can use the data presented herein with contaminant transport models (such as POLLUTE v7; Rowe and Booker 2004) to calculate contaminant escape through different types of landfill covers (or liners) and establish either concentrations in adjacent groundwater or unsaturated soil. Alternatively they can be used to calculate the mass flux of these contaminants through the cover/liner systems. The values given are considered to be suitable to assess sensitivity and for preliminary design. Since the results are for particular geomembranes, in cases where the results are critical to the success of a project, tests should be conducted on the specified material to confirm the parameters for

that specific material. Notwithstanding the limitations of this, like any experimental study, the results presented in this paper demonstrate that the coextruded EVOH geomembrane has a much greater capacity to minimize the permeation of the VOCs in a landfill than traditional cover materials such as HDPE or PVC.

Conclusions

This study examined the diffusive parameters of VOCs (benzene, toluene, ethylbenzene, and xylenes) migrating through two novel coextruded geomembranes (one with a polyamide barrier and one with an ethylene vinyl-alcohol barrier) and a standard 20-mil linear low-density polyethylene. Diffusion (D_g), partitioning (S_g), and permeation (P_g) coefficients were established for each

Table 8. Comparison of Aqueous Phase Permeation Coefficients with Those for 0.76-mm (30-mil) PVC Geomembrane

Contaminants	P_g (PVC) (10^{10} m ² s ⁻¹)	P_g (PVC)/ P_g (LLDPE) (-)	P_g (PVC)/ P_g (nylon) (-)	P_g (PVC)/ P_g (EVOH upper bound) (-)
Benzene	2.0	3–6	20–30	110
Toluene	5.1	4–9	35–45	170
Ethylbenzene	10	6–12	45	180
<i>m</i> & <i>p</i> -xylenes	9.5	5–10	40	200
<i>o</i> -xylene	6.5	4–8	30	165

Table 9. Comparison of Vapor Phase Permeation Coefficients with Those for 0.76-mm (30-mil) PVC Geomembrane

Contaminants	P_g (PVC) (10^{10} m ² s ⁻¹)	P_g (PVC)/ P_g (LLDPE) (-)	P_g (PVC)/ P_g (nylon) (-)	P_g (PVC)/ P_g (EVOH upper bound) (-)
Benzene	0.9	1	10	225
Toluene	2.9	2–4	20–30	360
Ethylbenzene	6.8	4–5	30–45	250
<i>m</i> & <i>p</i> -xylenes	7.0	5	30–35	330
<i>o</i> -xylene	4.5	4	20–35	250

Table 10. Comparison of Aqueous Phase Diffusion Coefficients of Coextruded Geomembranes to PVC, LLDPE, and HDPE Geomembranes

Contaminants	PVC ^a	LLDPE ^a	LLDPE	HDPE ^b	Nylon VBP15	LLDPE with EVOH
Thickness	(0.76 mm)	(0.76 mm)	(0.53 mm)	(2.0 mm)	(0.38 mm)	(0.53 mm)
Diffusion coefficient, D_g	(10^{13} m ² s ⁻¹)	(10^{13} m ² s ⁻¹)	(10^{13} m ² s ⁻¹)	(10^{13} m ² s ⁻¹)	(10^{13} m ² s ⁻¹)	(10^{13} m ² s ⁻¹)
Benzene	10.0	5.0	4.0	3.5	0.07–0.10	0.090
Toluene	9.3	4.5	3.0	3.0	0.11–0.14	0.085
Ethylbenzene	8.0	3.5	2.0	1.8	0.21	0.080
<i>m</i> & <i>p</i> -xylenes	7.0	3.0	2.0	1.7	0.22	0.080
<i>o</i> -xylene	5.0	2.5	2.0	1.5	0.20	0.075

^aResults from previous studies (McWatters and Rowe 2009).

^bResults from literature (Sangam and Rowe 2001).

Table 11. Comparison of Aqueous Phase Permeation Coefficients of Coextruded Geomembranes to PVC, LLDPE, and HDPE Geomembranes

Contaminants	PVC ^a	LLDPE ^a	LLDPE	HDPE ^b	Nylon VBP15	LLDPE with EVOH
Thickness	(0.76 mm)	(0.76 mm)	(0.53 mm)	(2.0 mm)	(0.38 mm)	(0.53 mm)
Permeability coefficient, P_g	($10^{10} \text{ m}^2 \text{ s}^{-1}$)	($10^{10} \text{ m}^2 \text{ s}^{-1}$)	($10^{10} \text{ m}^2 \text{ s}^{-1}$)	($-10^{10} \text{ m}^2 \text{ s}^{-1}$)	($10^{10} \text{ m}^2 \text{ s}^{-1}$)	($10^{10} \text{ m}^2 \text{ s}^{-1}$)
Benzene	1.3	1.0	0.7	0.1	0.6–0.8	0.018
Toluene	3.6	1.8	1.1	0.3	0.6–0.8	0.030
Ethylbenzene	7.8	1.6	0.8	0.5	0.5	0.056
<i>m</i> & <i>p</i> -xylenes	7.5	1.4	0.9	0.6	0.5	0.048
<i>o</i> -xylene	4.7	1.1	0.8	0.4	0.5	0.041

^aResults from previous studies (McWatters and Rowe 2009).

^bResults from literature (Sangam and Rowe 2001).

geomembrane in the aqueous and vapor phases. P_g values for the 0.53-mm (20-mil) thick LLDPE geomembrane were $(0.7\text{--}1.1) \times 10^{-10} \text{ m}^2 \text{ s}^{-1}$ for VOCs in the aqueous phase. The corresponding P_g values for the 0.38-mm (15-mil) thick geomembrane with a nylon barrier were $(0.07\text{--}0.22) \times 10^{-10} \text{ m}^2 \text{ s}^{-1}$ and those for 0.53-mm (20-mil) thick geomembrane with an EVOH barrier were $(0.018\text{--}0.056) \times 10^{-10} \text{ m}^2 \text{ s}^{-1}$ (aqueous phase). Results have also been presented for permeation of VOCs from the vapor phase.

Results for the overall permeation through the geomembrane were compared to a 0.76-mm (30-mil) thick PVC geomembrane. The LLDPE geomembrane had a permeation coefficient 3–12 times smaller (better, all other things being equal) than PVC for the aqueous phase and 1–5 times smaller than PVC for the vapor phase. The nylon geomembrane showed a 20–45-fold decrease in permeation coefficient in the aqueous phase and 10–45-fold decrease in the vapor phase over PVC. The geomembrane with the EVOH barrier showed the greatest improvement in reducing the mass flux of BTEX. The upper bound P_g values for the coextruded EVOH were of 110–200 times smaller than PVC for VOCs in the aqueous phase. For the vapor phase, the ratios were 225–360. Since these are upper bound values for EVOH, the relative performance is likely to be even better than indicated here. Thus the coextruded geomembranes reduced the diffusive mass flux of VOC contaminants significantly compared to traditional PVC and LLDPE liners. Results were also compared to a standard 2.0-mm thick HDPE geomembrane. The nylon geomembrane had similar P_g values to HDPE for ethylbenzene and xylenes. The EVOH geomembrane showed at least (remembering that the EVOH values are upper bounds) a 5–12-fold decrease in permeation coefficients when compared with HDPE, thereby improving the VOC diffusive barrier over the most commonly used geomembrane in landfill design.

Acknowledgments

The study was financially supported by Raven Industries. The value of discussion with Gary Kolbasuk is very gratefully acknowledged. The writers are also grateful to the Analytical Services Unit of Queen's University, Kingston, Canada for their support and use of their laboratory facilities.

References

Barone, F. S., Rowe, R. K., and Quigley, R. M. (1992). "A laboratory estimation of diffusion and adsorption coefficients for several volatile organics in a natural clayey soil." *J. Contam. Hydrol.*, 10, 225–250.

- Bouazza, A., and Vangpaisal, T. (2006). "Laboratory investigation of gas leakage rate through a GM/GCL composite liner due to a circular defect in the geomembrane." *Geotext. Geomembr.*, 24(2), 110–115.
- Bouazza, A., Vangpaisal, T., Abuel-Naga, H., and Kodikara, J. (2008). "Analytical modelling of gas leakage rate through a geosynthetic clay liner-geomembrane composite liner due to a circular defect in the geomembrane." *Geotext. Geomembr.*, 26(2), 122–129.
- Brachman, R. W. I., and Gudina, S. (2008a). "Gravel contacts and geomembrane strains for a GM/CCL composite liner." *Geotext. Geomembr.*, 26(6), 448–459.
- Brachman, R. W. I., and Gudina, S. (2008b). "Geomembrane strains from coarse gravel and wrinkles in a GM/GCL composite liner." *Geotext. Geomembr.*, 26(6), 488–497.
- Edil, Tuncer B. (2003). "A review of aqueous-phase VOC transport in modern landfill liners." *Waste Manage.*, 23, 561–571.
- El-Zein, A., and Rowe, R. K. (2008). "Impact on groundwater of concurrent leakage and diffusion of dichloromethane through geomembranes in landfill liners." *Geosynthet. Int.*, 15(1), 55–71.
- Gonzalez-Nunez, R., Padilla, H., De Kee, D., and Favis, B. D. (2001). "Barrier properties of polyamide-6/high density polyethylene blends." *Polym. Bull. (Berlin)*, 46, 323–330.
- Haxo, H. E. (1990). "Determining the transport through geomembranes of various permeant in different applications." *Geosynthetic testing for waste containment applications, STP 1081*, R. M. Koerner, ed., ASTM International, West Conshohocken, PA, 75–94.
- Kolbasuk, G. M. (1990). "Coextruded HDPE/VLDPE multilayer geomembranes." *Proc., 4th GRI Seminar on Landfill Closures: Geosynthetics, Interface Friction & New Developments*, 228–238.
- McWatters, R., and Rowe, R. K. (2007). "Diffusive migration of volatile organic compounds through PVC geomembranes." *Geosynthetics 2007, Proc. Environmental Conf.*, Wash., 106–120.
- McWatters, R., and Rowe, R. K. (2009). "Transport of volatile organic compounds through PVC and LLDPE geomembranes from both aqueous and vapour phases." *Geosynthet. Int.*, 16(6), 468–480.
- Montgomery, J. H., and Welkom, L. M. (1990). *Groundwater chemicals desk reference*, Lewis Publishers, Chelsea, MI, 106–120.
- Mueller, W., Jakob, I., Tatzky-Gerth, R., and August, H. (1998). "Solubilities, diffusion and partition coefficients of organic pollutants in HDPE geomembranes: Experimental results and calculations." *Proc., 6th Int. Conf. on Geosynthetics, Federal Institute for Materials Research and Testing*, BAM, Berlin, 239–248.
- Nefso, E. K., and Burns, S. E. (2007). "Comparison of the equilibrium sorption of five organic compounds to HDPE, PP, and PVC geomembranes." *Geotext. Geomembr.*, 25, 360–365.
- Park, J. K., and Nibras, M. (1993). "Mass flux of organic chemicals through polyethylene geomembranes." *Water Environ. Res.*, 65, 227–237.
- Peng, J. (1998). "Distribution of volatile contaminants between air and water." *Can. J. Civ. Eng.*, 25, 1091–1095.
- Pierson, P., and Barroso, M. (2002). "A pouch test for characterizing gas permeability of geomembranes." *Geosynthet. Int.*, 9(4), 345–372.
- Prasad, T. V., Brown, K. W., and Thomas, J. C. (1994). "Diffusion coef-

- ficients of organics in high density polyethylene (HDPE).” *Waste Manage. Res.*, 12(1), 61–71.
- Rowe, R. K. (1998). “Geosynthetics and the minimization of contaminant migration through barrier systems beneath solid waste.” *Proc., 6th Int. Conf. Geosynthetics*, Industrial Fabrics Association International, Roseville, MN, 27–103.
- Rowe, R. K. (2005). “Long-term performance of barrier systems.” *Geotechnique*, 55(9), 631–678.
- Rowe, R. K., and Booker, J. R. (2004). *POLLUTE v. 7—1D pollutant migration through a non-homogeneous soil*, GAEA Environmental Engineering, Whitby, Ont.
- Rowe, R. K., Caers, C. J., and Barone, F. (1988). “Laboratory determination of diffusion and distribution coefficients of contaminants using undisturbed clayey soil.” *Can. Geotech. J.*, 25(1), 108–118.
- Rowe, R. K., Hrapovic, L., and Kosaric, N. (1995b). “Diffusion of chloride and DCM through HDPE geomembrane.” *Geosynthet. Int.*, 2(3), 507–535.
- Rowe, R. K., Quigley, R. M., and Booker, J. R. (1995a). *Clayey barrier systems for waste disposal facilities*, Vol. 390, E & FN Spon (Chapman & Hall), London, Ont.
- Rowe, R. K., Quigley, R. M., Brachman, R. W. I., and Booker, J. R. (2004). *Barrier systems for waste disposal facilities*, 2nd Ed., Spon, London.
- Rowe, R. K., Rimal, S., and Sangam, H. P. (2009). “Ageing of HDPE geomembrane exposed to air, water and leachate at different temperatures.” *Geotext. Geomembr.*, 27(2), 137–151.
- Saidi, F., Touze-Foltz, N., and Goblet, P. (2008). “Numerical modelling of advective flow through composite liners in case of two interacting adjacent square defects in the geomembrane.” *Geotext. Geomembr.*, 26(2), 196–204.
- Sangam, H. P. (2001). “Performance of HDPE geomembrane liners in landfill applications.” Ph.D. thesis, Doctor of Engineering Science, Univ. of Western Ontario, Ont.
- Sangam, H. P., and Rowe, R. K. (2001). “Migration of dilute aqueous organic pollutants through HDPE geomembranes.” *Geotext. Geomembr.*, 19(6), 329–357.
- Sangam, H. P., and Rowe, R. K. (2005). “Effect of surface fluorination on diffusion through an HDPE geomembrane.” *J. Geotech. Geoenviron. Eng.* 131(6), 694–704.
- Stark, T. D., and Choi, H. (2005). “Methane gas migration through geomembranes.” *Geosynthet. Int.*, 12(2), 120–126.
- Take, W. A., Chappel, M. J., Brachman, R. W. I., and Rowe, R. K. (2007). “Quantifying geomembrane wrinkles using aerial photography and digital image processing.” *Geosynthet. Int.*, 14(4), 219–227.
- Thusyanthan, N. I., Madabhushi, S. P. G., and Singh, S. (2007). “Tension in geomembranes on landfill slopes under static and earthquake loading—Centrifuge study.” *Geotext. Geomembr.*, 25(2), 78–95.
- Tucker, W. A., and Nelken, L. H. (1982). “Diffusion coefficients in air and water.” *Handbook of Chemical Property Estimation Methods*, W. J. Lyman, W. F. Reehl, and D. H. Rosenblatt, eds., American Chemical Society, Washington, D.C.
- United States Environmental Protection Agency (U.S. EPA). (1996). *Method 8260: Volatile organic compounds by gas chromatography/mass spectrometry (GC/MS)*, U.S. EPA, Narragansett, R.I.
- United States Environmental Protection Agency (U.S. EPA). (2003). “Hazardous landfill gas.” *Federal Register: Rules and Regulations*, 68(No. 11), 2227–2242.
- Xiao, S., Moresoli, C., Bolvenkamp, J., and De Kee, D. (1997). “Sorption and permeation of organic environmental contaminants through PVC geomembranes.” *J. Appl. Polym. Sci.*, 63(9), 1189–1197.
- Yeh, J.-T., and Fan-Chiang, C.-C. (1996). “Permeation mechanisms of xylene in blow-molded bottles of pure polyethylene, polyethylene/polyamide and polyethylene/modified polyamide blends.” *J. Polym. Res.*, 3(4), 211–219.